One Functional Switch Mediates Reversible and Irreversible Inactivation of a Herpesvirus Protease†

Anson M. Nomura, Alan B. Marnett, Nobuhisa Shimba, Volker Dötsch, and Charles S. Craik*

Departments of Pharmaceutical Chemistry and Cellular and Molecular Pharmacology, University of California San Francisco, San Francisco, California 94143

Received November 18, 2005; Revised Manuscript Received January 20, 2006

ABSTRACT: Distinct mechanisms have evolved to regulate the function of proteolytic enzymes. Viral proteases in particular have developed novel regulatory mechanisms, presumably due to their comparatively rapid life cycles and responses to constant evolutionary pressure. Herpesviruses are a family of human pathogens that require a viral protease with a concentration-dependent zymogen activation involving folding of two α-helices and activation of the catalytic machinery, which results in formation of infectious virions. Kaposi's sarcoma-associated herpesvirus protease (KSHV Pr) is unique among the herpesvirus proteases in possessing aninere(in)-3 [(in)-380(thn)-3dimember whiers[(in)-380(thn)-carboxylia0(f)-245ial
M2id

The present study uses circular dichroism (CD), NMR, and a peptide-based phosphonate inhibitor of KSHV Pr to characterize the structural differences between the full-length monomeric, truncated monomeric, and dimeric KSHV Pr and to understand how protease activity is regulated by those conformational changes. Comparison of the dimer and monomer secondary structure using CD allows quantification of differences between the two structures. Measurement of inhibitor binding and reactivity separates the dimerization dependence of substrate binding and turnover on those structural changes. Dimerization controls the reversible activation of all herpesvirus proteases; however, KSHV has evolved a mechanism of irreversible inactivation by autolysis at the internal D-site. D-site cleavage removes helix 6 and leads to irreversible dissociation and inactivation of the resulting truncated protein, referred to as KSHV Pr Δ. The structural and functional consequences of autolytic cleavage are examined by comparison of the NMR chemical shifts and enzymatic activity of the truncated and full-length monomeric proteases. These experiments show that herpesvirus proteases have evolved a switch that stabilizes the transition state machinery, which KSHV Pr exploits at multiple points in the viral life cycle through two different structural rearrangements. These unique control mechanisms are compared to those of well-studied proteolytic enzymes with an emphasis on the similarities in the regulation of structurally diverse proteases.

MATERIALS AND METHODS

Recombinant Expression, Purification, and Quantification of KSHV Protease. A protease variant containing the S204G mutation that is stable to autolysis, referred to as wild-type (WT) protease, a variant containing both the M197D and S204G mutations, referred to as the monomeric or M197D protein, and the truncated protein, KSHV Pr Δ, were expressed in *Escherichia coli* and purified as previously described (*17*). Protease samples incorporating isotopically labeled Asp, Phe, Ile, Leu, Val, or Tyr were recombinantly expressed in *E. coli* DL39 using M9 media supplemented with the appropriate amino acids. Samples incorporating isotopically labeled Ala, Cys, His, Pro, or Arg were recombinantly expressed in *E. coli* strain BL21(DE3) in M9 media supplemented with all amino acids, nucleosides, and vitamins (*35*). Samples incorporating full ^{13}C and ^{15}N isotopic labeling or ^{2}H, ^{13}C, ^{15}N labeling were recombinantly expressed in *E. coli* BL21(DE3) either in M9 medium supplemented with 2 g/L ^{13}C-labeled glucose and 1 g/L ^{15}N-labeled ammonium chloride, in H_2O or D_2O, or in Silantes *E. coli* OD2 CDN media containing ^{2}H, ^{13}C, and ^{15}N. Protease concentrations were determined using a calculated $\epsilon_{280} = 0.931$ mg/mL for wild-type and M197D proteins, $\epsilon_{280} = 1.000$ mg/mL for Δ, and $\epsilon_{280} = 0.957$ mg/mL for inhibited wild-type protease covalently modified with the inhibitor acetyl-Pro-Val-Tyr-tBug-Gln-AlaP-$(OPh)_2$ after hydrolysis of the two phenoxy moieties. The inhibitor was synthesized both with and without a biotin moiety on the amino terminus as previously described (*33*).

Fluorescence Polarization. KSHV Pr variants were serially diluted from 10.0 to 0.006 μM in assay buffer (25 mM potassium phosphate, 150 mM NaCl, 1 mM dithiothreitol, 1 mM EDTA, pH 8.0) followed by addition of BODIPY-labeled inhibitor (20 nM) and placed in a 384-well plate yielding final protein concentrations of 5.0−0.003 μM and 10 nM fluorescent inhibitor concentration. The samples were allowed to equilibrate for 30 min at room temperature. Binding was then measured using fluorescence polarization (excitation 485 nm, emission 530 nm) on an Analyst AD (Molecular Devices). Polarization experiments were performed in triplicate. Data were analyzed using SigmaPlot 8.0 (SPSS, Chicago, IL), and the K_d values were obtained by fitting data to the equation $y = \min + [(\max - \min)/(1 + (x/K_d)^{\text{Hill slope}})]$.

Detection of Protease Inhibition by Streptavidin Blot. Wild-type or monomeric protease (37 μM) was incubated with the biotinylated phosphonate (200 μM) for 72 h at room temperature prior to SDS−PAGE separation. Protein was transferred to nitrocellulose for detection of the biotin moiety by streptavidin−HRP (Vectastain; Vector Labs).

Measurement of Protease Activity. Activity assays were performed in assay buffer (25 mM potassium phosphate, pH 8.0/150 mM potassium chloride/100 μM EDTA/1 mM 2-mercaptoethanol) at 30 °C. The Tyr-Val-tBug-Ala-ACC substrate was synthesized and purified as described (*36*), and substrate turnover was monitored for 1 h with an excitation wavelength of 380 nm and an emission wavelength of 460 nm. Protease samples were diluted into assay buffer and allowed to equilibrate for at least 1 h. The concentration of dimeric protease was calculated using the previously determined dissociation constant of 1.8 μM and the total concentration of protease using the equation previously derived (*33*).

NMR Backbone Resonance Assignments. NMR samples were prepared in NMR buffer (25 mM potassium phosphate, pH 7.0/0.1 mM EDTA/1 mM 2-mercaptoethanol) with D_2O added to 10% final concentration for deuterium lock. Uniformly labeled protease samples were 0.5−0.7 mM, while selectively labeled samples were between 0.25 and 0.7 mM. All NMR experiments were conducted at 27 °C on either a Bruker Avance 500 MHz, a DRX 600 MHz, or an Avance 800 MHz NMR instrument equipped with a triple resonance cryoprobe with *Z*-axis gradients. All proton chemical shifts were referenced to an internal DSS standard at 0 ppm. Carbon and nitrogen chemical shifts were indirectly referenced to the internal DSS standard using the ratios 0.251449537 and 0.101329118, respectively (*37*). Two-dimensional ^{1}H, ^{15}N heteronuclear single-quantum coherence (HSQC) spectra of M197D were collected with Ala, Arg, Asp, Cys, His, Ile, Leu, Lys, Phe, Tyr, Val, and uniformly ^{15}N-labeled samples. Two-dimensional ^{1}H, ^{15}N HNCO spectra were collected with uniformly ^{15}N-labeled samples with one of the amino acids, Ile, Leu, Phe, Pro, Tyr, or Val, ^{13}C labeled on the carbonyl carbon. Three-dimensional experiments for sequential backbone assignments were comprised of an HNCA, HN(CO)CA, HNCO, ^{1}H, ^{15}N NOESY HSQC (100 ms mixing time), TROSY HNCA, TROSY HN(CO)CA, and TROSY HNCACB (*38*). Average chemical shift differences between KSHV Pr M197D and KSHV Pr Δ were determined using the previously published equation, $\Delta_{av} = [(\Delta\delta^2_{HN} + \Delta\delta^2_{N}/25)/2]^{1/2}$ (*39*). All spectra were transformed using the XWINNMR software. Data visualization and spectral assignments used the XEASY (*40*) and Sparky (*41*) software packages.

Secondary Structure Measured by Circular Dichroism (CD). CD measurements were performed on a Jasco J-715

spectropolarimeter in 0.1 cm temperature-controlled quartz cuvettes at 27 °C. Protease samples were diluted into CD buffer (25 mM potassium phosphate, pH 8.0/1 mM 2-mercaptoethanol) to ~0.1 mg/mL and allowed to equilibrate for 1 h before measurements. Mean molar residue ellipticities were obtained after solvent spectrum subtraction and 10-fold signal averaging. Secondary structure content was estimated using the self-consistent method contained in the Dicroprot software (*42*, *43*).

Protein Structure Comparison and Visualization. Graphical representation of chemical shifts, CD, and binding curves were created using Kaleidagraph. All models use Pymol (*44*) to visualize the structure of KSHV Pr (PDB accession code 1FL1) (*25*). All KSHV Pr dimer secondary structure analysis is derived from the above referenced file.

RESULTS

Quantification of Structural Differences between the Monomer and Dimer of KSHV Pr. Previous experiments have demonstrated that herpesvirus proteases lose secondary structure upon dissociation and that this conformational change results in loss of enzymatic activity (*18*, *34*). A direct comparison between the monomer and dimer has been conducted through the use of an M197D mutation, which yields inactive monomers, and a hexapeptide diphenyl phosphonate covalent inhibitor, which stabilizes the protease dimer (*33*). Comparison of multiple engineered mutations in the KSHV Pr interfacial helix, adjacent to the active site and in the active site, which result in obligate monomers, has shown that loss of dimerization and activity is not linked to any specific point mutant, such as M197D (*18*; data not shown). The M197D point mutation has been shown to result in obligate monomers, which are structurally indistinct from wild-type monomers isolated at temperatures which allow dimer dissociation (*18*). In addition, a monomer containing the M197D substitution as well as a cross-link between helix 6 and the oxyanion loop has proteolytic activity (*34*). Taken together, these data strongly suggest that the presence of M197D does not directly disrupt catalysis. CD measurements of the monomeric KSHV Pr variant M197D, the equilibrium mixture of monomeric and dimeric wild-type KSHV Pr, and the completely dimeric inhibited KSHV Pr were collected and are shown in Figure 1a. Secondary structure predictions, based on these measurements, are listed in Table 1. A related herpesvirus protease and predicted secondary structure from X-ray structures are also listed for comparison. Monomeric KSHV Pr is composed of only 21% α-helix, which is in contrast to the 29% α-helix present in the equilibrium mixture of WT KSHV Pr, at low micromolar concentrations, and the 32% α-helix in completely dimeric KSHV Pr. The increase in α-helical content of the inhibited dimer, compared to the free dimer, is due to the weak dissociation constants of all herpesvirus proteases (1.8 μM for KSHV Pr). Therefore, CD measurements taken at concentrations near the dissociation constant, without the inhibitor, measure a mixture of monomers and dimers. Epstein−Barr virus protease (EBV Pr), a related γ-herpesvirus protease, is also composed of 29% α-helix at low micromolar concentrations (*26*). Analysis of the X-ray dimeric structures of KSHV Pr and EBV Pr shows that, when completely dimeric, both proteases should possess 31% α-helicity, consistent with the α-helical content of dimeric, inhibited KSHV Pr as measured by CD (*25*, *26*).

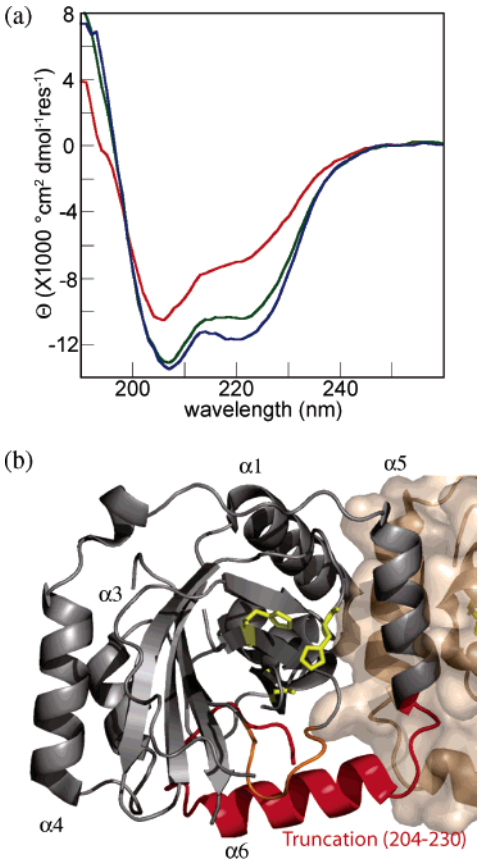

FIGURE 1: Comparison of dimeric and monomeric KSHV Pr. (a) Circular dichroism wavelength measurements of the full-length monomer (red), the equilibrium mixture of monomer and dimer at 3.0 μM (green), and the inhibitor-bound dimer (blue) measured at 27 °C. (b) Structure of KSHV Pr labeled with the active site (yellow), oxyanion hole loop (orange), truncated amino acids (red), and helices, including helix 5 and helix 6, which become disordered upon dissociation of the dimer.

Table 1: Secondary Structure Predictions

protease	oligomeric state	% α-helix	% β-strand	% other
KSHV Pr M197D	monomer	21	21	58
KSHV Pr WT	monomer + dimer	29	19	52
KSHV Pr WT, inhibited	dimer	32	18	50
KSHV Pr WT, predicted	dimer	31	26	43
EBV Pr WT	monomer + dimer	29	18	53
EBV Pr, predicted	dimer	31	23	46

Use of the inhibitor, which stabilizes the dimeric conformation of KSHV Pr (*33*), has allowed the direct comparison of the α-helical content between the monomeric and dimeric conformations of a herpesvirus protease, revealing a loss of 31% α-helicity upon dissociation.

Full-Length and Truncated KSHV Pr Bind but Cannot Cleave Substrate. CD confirmed earlier NMR experiments and directly measured the loss of α-helical content in the monomer relative to the dimer (*34*). Together, these results indicate that only helix 5 and helix 6, which are adjacent to the dimer interface as shown in Figure 1b, are affected by dimerization, while the β-barrel and areas distant from the interface are unperturbed by dissociation. These structural studies support earlier evidence that the conformational change is associated with disruption of the catalytic machin-

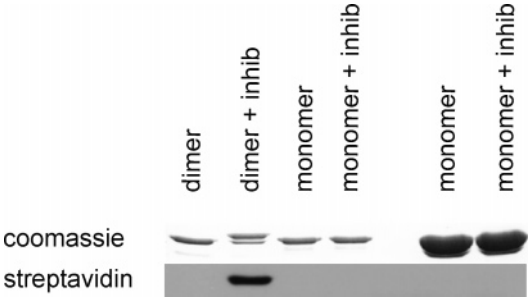

FIGURE 2: The KSHV protease dimer is catalytically active, and the monomer is inactive. Coomassie-stained gel of KSHV Pr variants with and without the addition of biotin-labeled hexapeptide phosphonate inhibitor. Lanes are KSHV Pr S204G − inhibitor, KSHV Pr S204G + inhibitor, KSHV Pr M197D − inhibitor, KSHV Pr M197D + inhibitor, KSHV Pr M197D − inhibitor overloaded, and KSHV Pr M197D + inhibitor overloaded. Immunoblot labeled with streptavidin−HRP with the same lanes as the Coomassie-stained gel above, showing only labeled KSHV Pr S204G dimer, which is shifted to a higher molecular weight due to inhibitor binding.

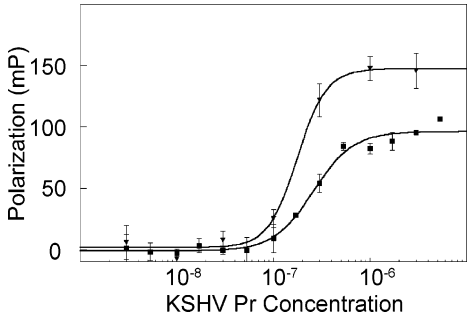

FIGURE 3: Monomeric herpesvirus proteases bind substrate. Polarization binding curves of KSHV Pr M197D (■) and KSHV Pr Δ (▼), using phosphonate inhibitor labeled with BODIPY. Binding curves have been normalized against inhibitor without protease. Substrate binding is unaffected by truncation (KSHV Pr M197D, K_d = 260 nM; KSHV Pr Δ, K_d = 180 nM).

ery but also indicate that substrate binding determinants may be unaffected by dimerization. Further experiments were conducted to clarify the effect of dimerization on substrate binding and turnover.

Incubation of KSHV Pr with the hexapeptide phosphonate inhibitor results in covalent modification of the active dimeric protease (*33*). This result showed that dimeric protease is capable of binding and reacting with substrate. Figure 2 shows a Coomassie-stained gel and streptavidin immunoblot of KSHV Pr variants with or without a biotin-labeled inhibitor. Full-length monomeric KSHV M197D is unable to react with the inhibitor, showing that the catalytic machinery in the monomer is disrupted. Binding of the inhibitor to WT KSHV Pr is evidenced by the shift in molecular weight of the protease in Figure 2 and the labeling of that band with streptavidin−HRP. KSHV Pr Δ also did not react with the inhibitor (data not shown). Increasing the amount of the monomeric KSHV Pr M197D does not result in any observable reaction with the biotin-labeled inhibitor, further showing that the monomer is unable to react with the transition state mimetic and is unable to turn over substrate.

BODIPY-labeled inhibitor was incubated with varying amounts of full-length monomeric KSHV Pr M197D or the truncated monomer to measure substrate binding, separate from turnover, by fluorescence polarization. These experiments, shown in Figure 3, reveal that both monomeric forms of KSHV Pr are able to bind the hexapeptide inhibitor. Although the inhibitor only contains the non-prime side of the substrate, the measured binding affinity is tighter than protease dimerization under similar conditions (K_d = 1.8 μM). Additionally, prime-side binding is known to contribute to substrate binding for herpesvirus proteases and would therefore increase the affinity of the substrate. Comparison of the binding affinity of the full-length (260 nM) and truncated monomers (180 nM) shows that autolysis does not substantially affect the binding affinity of the inhibitor. Therefore, both full-length and truncated monomeric KSHV Pr bind substrate with equivalent affinity but cannot catalyze proteolysis.

NMR Backbone Assignments for Characterization of Dimerization-Associated Structural Changes. A recent study used NMR-derived α-carbon chemical shifts to show that helix 5 and helix 6 are disordered in the monomer (*34*) while X-ray crystallography showed that both helices are well folded in the dimer (*25*). NMR was used to directly measure the conformations of both monomeric variants. The present study monitors the proton and nitrogen atoms, as well as the carbon atoms previously studied in the protein backbone, permitting comparison of the conformations of the dimer, full-length monomer, and truncated monomer. The poor solution behavior of KSHV Pr, coupled with its size, precluded the use of most traditional NMR triple resonance experiments for backbone assignments. Despite these limitations, utilization of selected triple resonance experiments, which show linear connectivity of residues through the primary sequence, and amino acid specific labeling (*45*−*48*) resulted in a total of 88% of the assignable backbone amide nitrogen and backbone amide protons in the full-length monomer being identified; 94% of the backbone α carbons and 77% of the backbone carbonyl carbons were also assigned. These alternative assignment methods did not result in the complete assignment of KSHV Pr but did present multiple sources of redundant assignment information, in an analogous manner to well-established purely pulse sequence-based methods, for those assignments that were made. Missing assignments were distributed throughout the protein and did not affect the overall interpretation of the structural changes. Similar analysis of KSHV Pr Δ resulted in 79% of the assignable backbone amide nitrogen and backbone amide protons and 94% of the backbone α carbons being assigned.

Comparison of Full-Length Monomeric and Truncated Inactive KSHV Pr. Both monomeric protease forms control proteolysis through the same functional mechanism; however, the conformational changes due to autolysis were still unknown. Comparison of the NMR structures of both full-length and truncated monomers was conducted to determine if the reversible and irreversible regulation of protease function relied on identical structural determinants. Figure 4a shows a comparison of the heteronuclear single-quantum coherence (HSQC) spectra of KSHV Pr M197D and KSHV Pr Δ. Each HSQC signal corresponds to an amide nitrogen and the attached proton. These signals are sensitive to the environment of each amino acid and can provide insights into changes in protein conformation and molecular interactions. Inspection of the spectral overlay shown in Figure 4a reveals that the spectra are virtually superimposable, indicat-

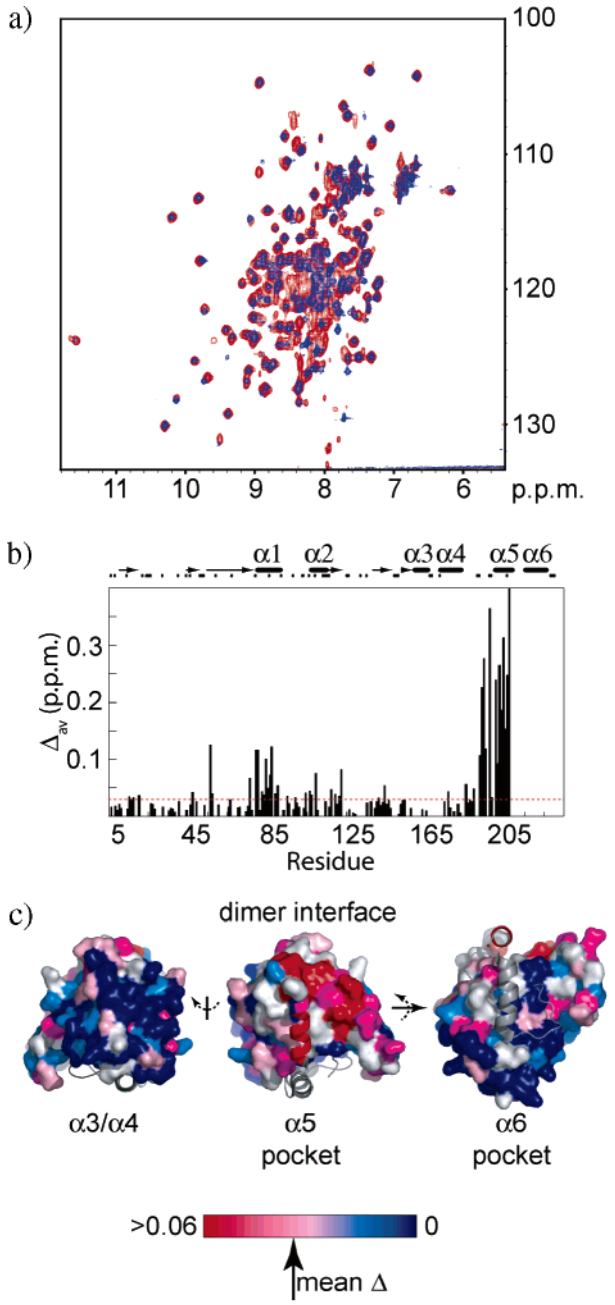

FIGURE 4: Comparison of KSHV Pr M197D and KSHV Pr Δ conformations. (a) Overlay of $^{1}H-^{15}N$ HSQC spectra of KSHV Pr M197D (red) and KSHV Pr Δ (blue), measured on a Bruker Avance 800 MHz instrument at 27 °C. (b) Plot of the averaged chemical shift difference for each residue. The average difference of all residues is shown as a dashed red line. The secondary structure of the KSHV Pr dimer is indicated above the graph (α-helices, ovals; β-strands, arrows). Unassigned residues are indicated as dashes below the secondary structure. (c) Averaged chemical shift changes shown on the KSHV Pr dimer structure, with colors indicated by key. Unassigned residues are shown in white. Monomer B has been removed for clarity, and helix 5 and helix 6 of monomer A are shown as ribbons.

ing that the two monomeric structures are nearly identical. Full-length protease contains 27 extra amino acids, which are located in the central region of the spectrum where unfolded amino acids are normally located. Assignment of KSHV Pr Δ was conducted, and Figure 4b plots the differences in each amino acid between the full-length and truncated monomers. Direct comparison of average amide chemical shifts confirms what cursory inspection of Figure 4a indicates; the structures of both monomeric protease forms are nearly identical. A majority of the amino acids have similar chemical shifts in both the full-length and truncated monomer, as evidenced by the fact that 79% of the assigned residues differ in chemical shift by less than the average of the entire protein. Only 35 of the assigned residues have differences in chemical shift, between the full-length and truncated monomers, which exceed the average difference for the entire protein. This fraction of the total amino acids accounts for the conformational changes that occur upon truncation.

Comparison of each chemical shift shows that the greatest differences between the full-length monomer and the truncation occur in helix 5, due to its proximity to the truncation site. Helix 5 is composed of residues 192−204. Truncation occurs between Ala203 and Ser204 and results in large chemical shift changes from Ala203 through Pro192. Large chemical shift differences extend beyond helix 5 in the loop connecting helix 5 to helix 4 through Asn188. The conformational changes in helix 5 and its preceding loop do not extend into helix 4 (residue 165−178), on the opposite side of the protein from the dimer interface. No amino acids in helix 3 or helix 4 have chemical shift differences between the two monomeric forms greater than the protein average, showing that no major conformational changes occur in this region of the protein. Additional locations with a high density of changes in chemical shifts between the two structures are located in helix 1 and helix 2, which both interact with helix 5 in the dimer, and together with helix 5 make up most of the dimer interface (*25*). Helix 1 contains greater than average chemical shift differences throughout the length of the helix, which extends from Ser73 to Arg91. The greatest chemical shift changes, and therefore the greatest conformational changes, occur in the amino terminus of helix 1, which is the region closest to helix 5. Helix 2, composed of Glu100 through Leu110, displays chemical shift differences greater than the protein average throughout its length. Additional small changes throughout the protein reflect slight differences in the overall fold; however, due to their small magnitudes relative to the changes in helix 1, helix 2, and helix 5, these changes do not represent the types of substantial changes linked to major conformational differences observed near the dimer disruption site as shown in Figure 4c. It is noteworthy that no changes of similar magnitude to those at the dimer interface occur in the regions of the protease which interact with helix 6 in the full-length dimer, indicating that these regions do not undergo large changes between the two monomeric forms. Comparison of the chemical shifts of full-length monomeric KSHV Pr M197D and the 203 amino acid C-terminal truncated KSHV Pr Δ shows isolated differences in structure centered around helix 5, with the remainder of both monomers assuming similar structures.

Dissociation of dimeric herpesvirus proteases leads to destabilization of helix 5 and helix 6. This unfolding event results in loss of the ability to carry out catalytic turnover with retention of the capacity for substrate binding. Autolysis of 27 amino acids, a second mode of enzymatic control, removes helix 6 and disrupts the dimer interface relative to the full-length monomer but does not perturb the remainder of the protein. Truncation also impairs catalytic turnover without disturbing substrate binding relative to the full-length

monomer. Therefore, both dissociation and truncation regulate enzymatic activity through similar structural elements and one functional mechanism.

DISCUSSION

Proteases are widespread enzymes that are often tightly regulated due to the catastrophic consequences that result from unchecked proteolysis. Activation and inactivation of proteolysis occur through multiple mechanisms including limited proteolysis, cofactor binding, inhibition, and oligomerization. The unique dimerization- and truncation-linked conformational changes in herpesvirus proteases result in enzymatic regulation through a functional mechanism that is used by many well-known proteolytic systems, specifically transition state stabilization.

Previous studies have shown that herpesvirus proteases are regulated by a dimerization-linked conformational change that disrupts the oxyanion loop necessary for transition state stabilization (*18*, *32*−*34*). Dimerization induces the folding of helix 5 and helix 6, which stabilize the oxyanion hole and contribute to the surprisingly weak binding affinity of these proteases. This conformational change has been quantified through CD measurements that compare a completely dimeric, inhibited protease to the obligate monomeric KSHV Pr M197D. The monomer is shown to contain 31% less α-helicity than the dimer, which is in good agreement with previous NMR studies. This comparison was possible because a transition state mimetic covalently modifies the active site and stabilizes the dimer (*33*). This phosphonate inhibitor was also useful for understanding the dimerization-associated regulation of KSHV Pr function.

The model of dimerization-dependent regulation was divided into two possible regulatory mechanisms: substrate binding and turnover. The isolated dimerization-linked structural changes shown by CD and NMR were expected to only influence substrate turnover; however, it was possible that perturbation of binding determinants could also occur. Fluorescence polarization binding measurements using a transition state mimetic show that monomeric herpesvirus proteases possess a stronger affinity for substrate binding than dimerization. In stark contrast, covalent labeling experiments with the inhibitor and monomeric protease, to test catalytic turnover, revealed a tight link between dimerization and bond cleavage, indicating that monomeric proteases contain disrupted catalytic machinery. These experiments emphasize the importance of the helix 6−oxyanion loop interaction to the mechanism of enzyme regulation. Previous experiments with cytomegalovirus protease (CMV Pr) have shown that perturbation of the dimer interface leads to a reduction in catalytic turnover but not substrate binding (*32*). This earlier method for assaying enzymes with low proteolytic activity could not be implemented with monomeric herpesvirus proteases due to the immeasurably low activity of the monomer relative to even mutant dimers. The use of fluorescence polarization and inhibitor labeling allows the functional characterization of even completely inactive monomeric and truncated herpesvirus proteases but would not be appropriate for the characterization of active species.

KSHV Pr is unique among the herpesvirus proteases in that it possesses an inactivating autolysis site within the interfacial helix 5 (*17*). Cleavage at this site removes the last turn of helix 5 and all of helix 6, resulting in a completely inactive monomeric species. This cleavage event occurs naturally and represents an irreversible inactivation of the enzyme. The effects of truncation on the structure of KSHV Pr were not clearly known, although earlier CD measurements had shown that the protein does not become completely unfolded (*17*). Chemical shift changes between the full-length and truncated monomers show that significant conformational changes occur in helix 5 and extend from the cleavage site at Ala203 beyond helix 5 into the loop connecting helix 4 and helix 5. Helix 5 and the preceding loop assume two different conformations in the full-length and truncated monomers. This difference may be due to the full-length monomeric helix 5, although unwound, continuing to interact with the main body of the protein, while the remainder of helix 5 and the preceding loop in the truncation do not retain this interaction. Additionally, large changes in the conformation of helix 1 and helix 2 are also evident in the truncation. These differences may indicate a shift in the packing of helix 1 relative to the rest of the protein, which would also account for the differences in helix 2, as the two helices are connected through a loop. The structural differences between the truncated and full-length monomers are limited to the dimer interface and adjacent areas. Therefore, the differences between the two monomeric forms are restricted to the same structural elements responsible for the dimerization-associated regulation of KSHV Pr.

Beyond these specific, localized differences, it is noteworthy that the overall structures of the two monomeric protease forms are not drastically different. Of special interest is the lack of large differences between the full-length and truncated protease binding pockets for helix 6, which are the surfaces through which helix 6 stabilizes the oxyanion hole. KSHV Pr Δ does not possess a helix 6; therefore, the similarity between both monomeric forms indicates that helix 6 does not significantly interact with the main body of the protein in the context of the full-length monomer. This supports earlier evidence of disorder in this region upon disruption of dimerization (*32*, *34*) and further defines the conformational changes linked to dimerization and activation.

Fluorescence polarization measurements and inhibitor binding assays of KSHV Pr Δ show that truncation does not affect substrate binding relative to the full-length monomer and that KSHV Pr Δ is also unable to turn over substrate. This similarity is expected, based on the NMR comparison of the two forms. Substrate binding is known to be mediated through the β-barrel and loops distant from the dimer interface, which are not affected by truncation, and KSHV Pr Δ should therefore bind the inhibitor with equivalent affinity to the full-length monomer. KSHV Pr appears to take advantage of the mechanism already in place for protease activation to also inactivate the enzyme through autolysis. Therefore, irreversible inactivation of KSHV Pr through autolytic truncation and reversible activation and inactivation of herpesvirus proteases by dimerization, two very different structural changes, both regulate enzymatic activity through the functional mechanism of transition state stabilization mediated by the helix 6−oxyanion loop interaction.

Spatial and temporal restrictions of proteolytic activity are not limited to herpesvirus proteases. Although herpesvirus proteases use a unique conformational change to regulate

activity, the functional mechanisms employed are used by other structurally unrelated proteases. KS is the most common cancer in AIDS patients, and the viruses responsible for both of these devastating diseases, although structurally unrelated, share similar functional regulatory mechanisms. HIV protease is also regulated by dimerization and contains inactivating internal autolysis sites (*49*−*51*). Regulation of HIV protease is necessary for virion formation. Perturbation of dimerization-linked activation results in premature processing of viral proteins, disruption of the viral life cycle, and cellular toxicity (*52*). Cellular toxicity is thought to result from cleavage of cellular proteins by the unregulated HIV protease, which is normally controlled by dimerization and autolytic inactivation. A necessity for autolysis has been shown in a related herpesvirus protease. The importance of D-site cleavage to the KSHV Pr lytic cycle is currently unknown; however, two different autolysis sites in CMV Pr have been shown to be important for virion formation and infectivity (*53*). Prevention of autolysis results in a 90% reduction in virus production. Although these two sites do not correspond to the D-site, one site may result in loss of helix 5 and helix 6 in the same way as D-site cleavage.

Herpesvirus protease regulation also shares characteristics with many nonviral proteases including trypsin, one of the most extensively studied proteases. Dimerization of herpesvirus proteases stabilizes the oxyanion loop, and in a similar fashion, the conversion of trypsinogen to trypsin also results in the organization of the oxyanion hole. Oxyanion hole stabilization is a mechanism of protease regulation which is widely utilized. Trypsin and other pancreatic proteases also possess inactivating autolysis sites, which have been shown to be important in the proper spatial regulation of activity. Similar parallels can be drawn between the control of KSHV Pr and the complement convertases, caspases, and coagulation proteases. These comparisons show that although proteases assume diverse structures, they can be regulated by a limited set of unifying mechanisms.

ACKNOWLEDGMENT

We thank Vladimir Basus, Frank Löhr, and Mark Kelly for technical assistance with NMR experiments.

SUPPORTING INFORMATION AVAILABLE

One table listing the amide nitrogen and amide proton chemical shifts of KSHV Pr M197D and KSHV Pr Δ. This material is available free of charge via the Internet at http://pubs.acs.org.

REFERENCES

1. Chang, Y., Cesarman, E., Pessin, M. S., Lee, F., Culpepper, J., Knowles, D. M., and Moore, P. S. (1994) Identification of herpesvirus-like DNA sequences in AIDS-associated Kaposi's sarcoma, *Science 266*, 1865−1869.
2. Kedes, D. H., Operskalski, E., Busch, M., Kohn, R., Flood, J., and Ganem, D. (1996) The seroepidemiology of human herpesvirus 8 (Kaposi's sarcoma-associated herpesvirus): distribution of infection in KS risk groups and evidence for sexual transmission, *Nat. Med. 2*, 918−924.
3. Moore, P. S., Gao, S. J., Dominguez, G., Cesarman, E., Lungu, O., Knowles, D. M., Garber, R., Pellett, P. E., McGeoch, D. J., and Chang, Y. (1996) Primary characterization of a herpesvirus agent associated with Kaposi's sarcomae, *J. Virol. 70*, 549−558.
4. Preston, V. G., Coates, J. A., and Rixon, F. J. (1983) Identification and characterization of a herpes simplex virus gene product required for encapsidation of virus DNA, *J. Virol. 45*, 1056−1064.
5. Preston, V. G., Rixon, F. J., McDougall, I. M., McGregor, M., and al Kobaisi, M. F. (1992) Processing of the herpes simplex virus assembly protein ICP35 near its carboxy terminal end requires the product of the whole of the UL26 reading frame, *Virology 186*, 87−98.
6. Register, R. B., and Shafer, J. A. (1996) A facile system for construction of HSV-1 variants: site directed mutation of the UL26 protease gene in HSV-1, *J. Virol. Methods 57*, 181−193.
7. Rixon, F. J., and McNab, D. (1999) Packaging-competent capsids of a herpes simplex virus temperature-sensitive mutant have properties similar to those of in vitro-assembled procapsids, *J. Virol. 73*, 5714−5721.
8. Newcomb, W. W., Trus, B. L., Cheng, N., Steven, A. C., Sheaffer, A. K., Tenney, D. J., Weller, S. K., and Brown, J. C. (2000) Isolation of herpes simplex virus procapsids from cells infected with a protease-deficient mutant virus, *J. Virol. 74*, 1663−1673.
9. Weinheimer, S. P., McCann, P. J., III, O'Boyle, D. R., Jr., Stevens, J. T., Boyd, B. A., Drier, D. A., Yamanaka, G. A., DiIanni, C. L., Deckman, I. C., and Cordingley, M. G. (1993) Autoproteolysis of herpes simplex virus type 1 protease releases an active catalytic domain found in intermediate capsid particles, *J. Virol. 67*, 5813−5822.
10. Robertson, B. J., McCann, P. J., III, Matusick-Kumar, L., Newcomb, W. W., Brown, J. C., Colonno, R. J., and Gao, M. (1996) Separate functional domains of the herpes simplex virus type 1 protease: evidence for cleavage inside capsids, *J. Virol. 70*, 4317−4328.
11. Welch, A. R., Woods, A. S., McNally, L. M., Cotter, R. J., and Gibson, W. (1991) A herpesvirus maturational proteinase, assemblin: identification of its gene, putative active site domain, and cleavage site, *Proc. Natl. Acad. Sci. U.S.A. 88*, 10792−10796.
12. Donaghy, G., and Jupp, R. (1995) Characterization of the Epstein−Barr virus proteinase and comparison with the human cytomegalovirus proteinase, *J. Virol. 69*, 1265−1270.
13. Unal, A., Pray, T. R., Lagunoff, M., Pennington, M. W., Ganem, D., and Craik, C. S. (1997) The protease and the assembly protein of Kaposi's sarcoma-associated herpesvirus (human herpesvirus 8), *J. Virol. 71*, 7030−7038.
14. Gao, M., Matusick-Kumar, L., Hurlburt, W., DiTusa, S. F., Newcomb, W. W., Brown, J. C., McCann, P. J., III, Deckman, I., and Colonno, R. J. (1994) The protease of herpes simplex virus type 1 is essential for functional capsid formation and viral growth, *J. Virol. 68*, 3702−12.
15. Baum, E. Z., Bebernitz, G. A., Hulmes, J. D., Muzithras, V. P., Jones, T. R., and Gluzman, Y. (1993) Expression and analysis of the human cytomegalovirus UL80-encoded protease: identification of autoproteolytic sites, *J. Virol. 67*, 497−506.
16. DiIanni, C. L., Drier, D. A., Deckman, I. C., McCann, P. J., III, Liu, F., Roizman, B., Colonno, R. J., and Cordingley, M. G. (1993) Identification of the herpes simplex virus-1 protease cleavage sites by direct sequence analysis of autoproteolytic cleavage products, *J. Biol. Chem. 268*, 2048−2051.
17. Pray, T. R., Nomura, A. M., Pennington, M. W., and Craik, C. S. (1999) Auto-inactivation by cleavage within the dimer interface of Kaposi's sarcoma-associated herpesvirus protease, *J. Mol. Biol. 289*, 197−203.
18. Pray, T. R., Reiling, K. K., Demirjian, B. G., and Craik, C. S. (2002) Conformational change coupling the dimerization and activation of KSHV protease, *Biochemistry 41*, 1474−1482.
19. Chen, P., Tsuge, H., Almassy, R. J., Gribskov, C. L., Katoh, S., Vanderpool, D. L., Margosiak, S. A., Pinko, C., Matthews, D. A., and Kan, C. C. (1996) Structure of the human cytomegalovirus protease catalytic domain reveals a novel serine protease fold and catalytic triad, *Cell 86*, 835−843.
20. Tong, L., Qian, C., Massariol, M. J., Bonneau, P. R., Cordingley, M. G., and Lagace, L. (1996) A new serine-protease fold revealed by the crystal structure of human cytomegalovirus protease, *Nature 383*, 272−275.
21. Qiu, X., Culp, J. S., DiLella, A. G., Hellmig, B., Hoog, S. S., Janson, C. A., Smith, W. W., and Abdel-Meguid, S. S. (1996) Unique fold and active site in cytomegalovirus protease, *Nature 383*, 275−279.
22. Shieh, H. S., Kurumbail, R. G., Stevens, A. M., Stegeman, R. A., Sturman, E. J., Pak, J. Y., Wittwer, A. J., Palmier, M. O., Wiegand, R. C., Holwerda, B. C., and Stallings, W. C. (1996) Three-

dimensional structure of human cytomegalovirus protease, *Nature 383*, 279−282.
23. Hoog, S. S., Smith, W. W., Qiu, X., Janson, C. A., Hellmig, B., McQueney, M. S., O'Donnell, K., O'Shannessy, D., DiLella, A. G., Debouck, C., and Abdel-Meguid, S. S. (1997) Active site cavity of herpesvirus proteases revealed by the crystal structure of herpes simplex virus protease/inhibitor complex, *Biochemistry 36*, 14023−14029.
24. Qiu, X., Janson, C. A., Culp, J. S., Richardson, S. B., Debouck, C., Smith, W. W., and Abdel-Meguid, S. S. (1997) Crystal structure of varicella-zoster virus protease, *Proc. Natl. Acad. Sci. U.S.A. 94*, 2874−2879.
25. Reiling, K. K., Pray, T. R., Craik, C. S., and Stroud, R. M. (2000) Functional consequences of the Kaposi's sarcoma-associated herpesvirus protease structure: regulation of activity and dimerization by conserved structural elements, *Biochemistry 39*, 12796−12803.
26. Buisson, M., Hernandez, J. F., Lascoux, D., Schoehn, G., Forest, E., Arlaud, G., Seigneurin, J. M., Ruigrok, R. W., and Burmeister, W. P. (2002) The crystal structure of the Epstein−Barr virus protease shows rearrangement of the processed C terminus, *J. Mol. Biol. 324*, 89−103.
27. Darke, P. L., Cole, J. L., Waxman, L., Hall, D. L., Sardana, M. K., and Kuo, L. C. (1996) Active human cytomegalovirus protease is a dimer, *J. Biol. Chem. 271*, 7445−7449.
28. Margosiak, S. A., Vanderpool, D. L., Sisson, W., Pinko, C., and Kan, C. C. (1996) Dimerization of the human cytomegalovirus protease: kinetic and biochemical characterization of the catalytic homodimer, *Biochemistry 35*, 5300−5307.
29. Schmidt, U., and Darke, P. L. (1997) Dimerization and activation of the herpes simplex virus type 1 protease, *J. Biol. Chem. 272*, 7732−7735.
30. Cole, J. L. (1996) Characterization of human cytomegalovirus protease dimerization by analytical centrifugation, *Biochemistry 35*, 15601−15610.
31. Holwerda, B. (1999) Activity in monomers of human cytomegalovirus protease, *Biochem. Biophys. Res. Commun. 259*, 370−373.
32. Batra, R., Khayat, R., and Tong, L. (2001) Molecular mechanism for dimerization to regulate the catalytic activity of human cytomegalovirus protease, *Nat. Struct. Biol. 8*, 810−817.
33. Marnett, A. B., Nomura, A. M., Shimba, N., Ortiz de Montellano, P. R., and Craik, C. S. (2004) Communication between the active sites and dimer interface of a herpesvirus protease revealed by a transition-state inhibitor, *Proc. Natl. Acad. Sci. U.S.A. 101*, 6870−6875.
34. Nomura, A. M., Marnett, A. B., Shimba, N., Dötsch, V., and Craik, C. S. (2005) Induced structure of a helical switch as a mechanism to regulate enzymatic activity, *Nat. Struct. Mol. Biol. 12*, 1019−1020.
35. Cheng, H., Westler, W. M., Xia, B., Oh, B. H., and Markley, J. L. (1995) Protein expression, selective isotopic labeling, and analysis of hyperfine-shifted NMR signals of Anabaena 7120 vegetative [2Fe-2S]ferredoxin, *Arch. Biochem. Biophys. 316*, 619−634.
36. Harris, J. L., Backes, B. J., Leonetti, F., Mahrus, S., Ellman, J. A., and Craik, C. S. (2000) Rapid and general profiling of protease specificity by using combinatorial fluorogenic substrate libraries, *Proc. Natl. Acad. Sci. U.S.A. 97*, 7754−7759.
37. Wishart, D. S., Bigam, C. G., Yao, J., Abildgaard, F., Dyson, H. J., Oldfield, E., Markley, J. L., and Sykes, B. D. (1995) ^{1}H, ^{13}C and ^{15}N chemical shift referencing in biomolecular NMR, *J. Biomol. NMR 6*, 135−140.
38. Salzmann, M., Pervushin, K., Wider, G., Senn, H., and Wüthrich, K. (1998) TROSY in triple-resonance experiments: new perspectives for sequential NMR assignment of large proteins, *Proc. Natl. Acad. Sci. U.S.A. 95*, 13585−13590.
39. Grzesiek, S., Stahl, S. J., Wingfield, P. T., and Bax, A. (1996) The CD4 determinant for downregulation by HIV-1 Nef directly binds to Nef. Mapping of the Nef binding surface by NMR, *Biochemistry 35*, 10256−10261.
40. Bartels, C., Xia, T.-H., Billeter, M., Güntert, P., and Wüthrich, K. (1995) The program XEASY for computer-supported NMR spectral analysis of biological macromolecules, *J. Biomol. NMR 6*, 1−10.
41. Goddard, T. D., and Kneller, D. G. SPARKY 3, University of California, San Francisco.
42. Sreerama, N., and Woody, R. W. (1993) A self-consistent method for the analysis of protein secondary structure from circular dichroism, *Anal. Biochem. 209*, 32−44.
43. Deleage, G., and Geourjon, C. (1993) An interactive graphic program for calculating the secondary structure content of proteins from circular dichroism spectrum, *Comput. Appl. Biosci. 9*, 197−199.
44. DeLano, W. L. (2002) The PyMOL Molecular Graphics System, DeLano Scientific, San Carlos, CA (http://www.pymol.org).
45. Hibler, D. W., Harpold, L., Dell'Acqua, M., Pourmotabbed, T., Gerlt, J. A., Wilde, J. A., and Bolton, P. H. (1989) Isotopic labeling with hydrogen-2 and carbon-13 to compare conformations of proteins and mutants generated by site-directed mutagenesis, I, *Methods Enzymol. 177*, 74−86.
46. Lee, K. M., Androphy, E. J., and Baleja, J. D. (1995) A novel method for selective isotope labeling of bacterially expressed proteins, *J. Biomol. NMR 5*, 93−96.
47. McIntosh, L. P., and Dahlquist, F. W. (1990) Biosynthetic incorporation of ^{15}N and ^{13}C for assignment and interpretation of nuclear magnetic resonance spectra of proteins, *Q. Rev. Biophys. 23*, 1−38.
48. Muchmore, D. C., McIntosh, L. P., Russell, C. B., Anderson, D. E., and Dahlquist, F. W. (1989) Expression and nitrogen-15 labeling of proteins for proton and nitrogen-15 nuclear magnetic resonance, *Methods Enzymol. 177*, 44−73.
49. Rose, J. R., Salto, R., and Craik, C. S. (1993) Regulation of autoproteolysis of the HIV-1 and HIV-2 proteases with engineered amino acid substitutions, *J. Biol. Chem. 268*, 11939−11945.
50. Tomasselli, A. G., Mildner, A. M., Rothrock, D. J., Sarcich, J. L., Lull, J., Leone, J., and Heinrikson, R. (1995) Site-directed mutagenesis of HIV-1 protease: generation of mutant proteases with increased stability to autodigestion, *Adv. Exp. Med. Biol. 362*, 473−477.
51. Tomasselli, A. G., Mildner, A. M., Rothrock, D. J., Sarcich, J. L., Lull, J., Leone, J., and Heinrikson, R. L. (1995) Mutants of HIV-1 protease with enhanced stability to autodegradation, *Adv. Exp. Med. Biol. 362*, 387−398.
52. Krausslich, H. G. (1991) Human immunodeficiency virus proteinase dimer as component of the viral polyprotein prevents particle assembly and viral infectivity, *Proc. Natl. Acad. Sci. U.S.A. 88*, 3213−3217.
53. Loveland, A. N., Chan, C. K., Brignole, E. J., and Gibson, W. (2005) Cleavage of human cytomegalovirus protease pUL80a at internal and cryptic sites is not essential but enhances infectivity, *J. Virol. 79*, 12961−12968.

BI0523658